Simulation Studies on the Characterization of Cerenkov Images by Fractal and Wavelet Parameters *

A. Haungs[1] †, A.K. Razdan[2], C.L. Bhat[2], R.C. Rannot[2], and H. Rebel[1]
[1] *Forschungszentrum Karlsruhe, Institut für Kernphysik, D-76021 Karlsruhe, Germany*
[2] *Bhabha Atomic Research Centre, Nuclear Research Laboratory, Mumbai - 400 085, India*

Abstract

Based on Monte Carlo simulations using the CORSIKA code, it is shown that Cerenkov images produced by ultrahigh energy γ-rays and cosmic ray nuclei (proton, Neon and Iron) have a fractal nature. The resulting multifractal and wavelet moments as inputs to a properly-trained artificial neural network are found to provide an efficient characterization scheme of the cosmic EAS primaries.

1 Introduction:

The atmospheric Cerenkov imaging technique reflects the current state-of-art for the observation of γ-rays in the TeV region. Apart from performing γ-ray astronomy investigations, this technique may hopefully pave the way for set in imaging Cerenkov telescopes eventually in a supplementary mode of operation for independent cosmic-ray mass-composition studies in the ultra-high energy region – an important problem of its own right. Motivated by this topic, we investigate here the possibility of subjecting the Cerenkov image data to perhaps more general, albeit as-yet untried, multifractal and wavelet analyses of deriving independent parameters which can supplement the presently-in-use Hillas moments for event-characterization. The paper discusses here first results of exploratory studies, based on Cerenkov image data simulated for the Imaging Element of the 4-element TACTIC (TeV Atmospheric Cerenkov Telescope with an Imaging Camera) array, using the CORSIKA air-shower code (Heck et al. 1998).

2 TACTIC:

The TACTIC instrument consists of an array of 4 atmospheric Cerenkov elements each using a tessellated optical collector of $9.5\,\mathrm{m}^2$ light collection area and a synchronized, computer-controlled alt-azimuth drive system. The central (imaging) element (IE) of this compact telescope array is located at the centroid of an equilateral triangle of $20\,$m-side and the 3 Vertex Elements (VE) are placed at the vertices of this triangular configuration (Bhatt et al. 1997). The IE has a fast photomultiplier tube (PMT)-based 349-pixel Imaging Camera in its focal-plane, covering a field-of-view (FoV) of $\sim 6^\circ \times 6^\circ$ truncated squarewith a pixel resolution of $\sim 0.31^\circ$ diameter. The VE's front-end instrumentation, apart from yielding a significantly lower trigger threshold energy for the VE's, provides information on the polarization state, spectral content and time-profile of the recorded ACE. Extensive Monte Carlo simulation studies are presently underway to provide specific guidelines for optimizing event characterization strategies and thereby enable this instrument to carry out VHE γ-ray astronomy and UHE cosmic-ray mass-composition investigations through the atmospheric Cerenkov detection route.

3 CORSIKA-based Cerenkov Image data-bases:

The data-bases for carrying out the present feasibility studies were generated using the CORSIKA (Version 4.5) air-shower code (Heck et al. 1998) with Cerenkov option, and the use of the high energy interaction model VENUS and the model GHEISHA for interactions at lower energies ($\mathrm{E}_{lab} < 80\,$GeV). A rectangular matrix of 60×4 detector elements, each $5\,\mathrm{m} \times 5\,\mathrm{m}$ in dimensions, is folded into the CORSIKA simulation programme

* The work is embedded in the Indian-German bilateral agreement of scientific-technical cooperation (WTZ INI-205).
† corresponding author; e-mail: haungs@ik3.fzk.de

for this purpose, in conformity with the actual geometrical configuration of the TACTIC array and the size of its 4 light-collectors. The Cerenkov data bases of 100 showers each for γ-rays, proton and Neon and Iron nuclei have been generated. These simulated data bases are valid for the altitude (1700 m) and magnetic field values of Gurushikhar, Mt. Abu, the permanent location of the TACTIC in the Western Indian state of Rajasthan. The zenith angle Θ of the primary is fixed at 40° for gamma and $40^\circ \pm 2^\circ$ for protons, Neon and Iron, larger Θ being preferred to achieve twin benefits of a higher primary threshold energy and a larger effective collection area. γ-rays of energy 50 TeV and protons, Neon and Iron nuclei of 100 TeV energy (the factor of two higher energy for nuclear-progenitors being chosen to have roughly comparable average Cerenkov photon densities in all the 4 cases) have been considered. To keep computer time and the Cerenkov photon file size within manageable limits for a given event, the Cerenkov photons are generated in the restricted wavelength region, $\lambda \sim (300 - 320)$ nm. Cerenkov photons likely to be received at a given element with λ outside the above-referred sample window are generated off-line, using the well-known Cerenkov radiation spectral law $\sim \lambda^{-2}$. Other exercises done subsequently in the off-line mode include (i) taking proper account of the λ-dependent atmospheric extinction suffered by the individual Cerenkov photons emitted in the overall wavelength interval $\lambda \sim (300 - 600)$ nm, (ii) ray-tracing Cerenkov photons, incident on each 60 cm-diameter facet of the IE mirror into the focal-plane of the light receiver, and (iii) deriving the number of photo-electrons (PE) likely to be registered by each of the 349 photomultiplier (PMT) pixels of the IE camera after accounting for the reflection coefficient of the mirror and the quantum efficiency of the PMT pixels. Each of these 256 pixels, (which also include the pixels with information on the simulated Cerenkov image) have been injected with a photomultiplier noise component ~ 4 PE. The noise injected in the image follows Poissonian distribution.

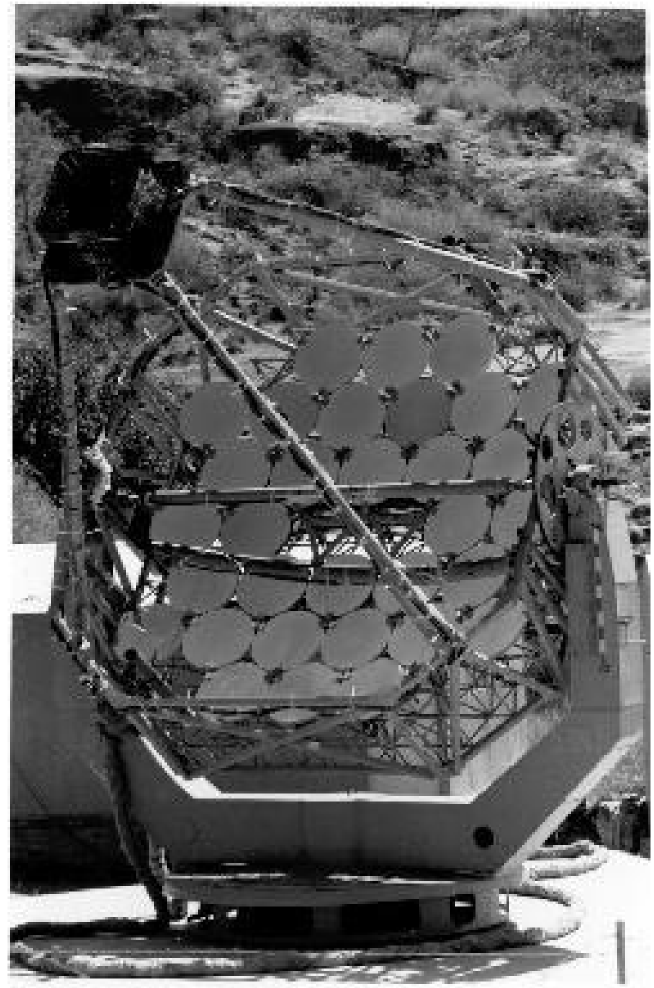

Figure 1: Photograph of the TACTIC central telescope installed at Gurushikar on Mt. Abu, Rajasthan, India (1700 m a.s.l.).

4 Imaging Parametrisation:

4.1 Multifractals: Fractals are structures which display a self similar behavior, and the fractal nature is quantitatively characterized by fractal dimensions. It is possible to calculate multifractal moments which quantify structures of multidimensional density distributions (Aharony 1990). In anticipation of the requirements of the associated analysis procedure, only the square-grid, comprising the innermost 16 x 16 pixels of the TACTIC Imaging camera, has been considered. Only images with a total number of $\geq$ 1800 PE have been used. We have calculated multifractal moments of each simulated Cerenkov image by dividing the image into M = 4, 16, 64 and 256 equally sized parts and by calculating the number of photoelectrons in each part. M is related to the fractal scale-length ν by $M = 2^\nu$.

The multifractal moments given by the following expression have been computed $G_q(M) = \sum_{j=1}^{M}(k_j/N)^q, N \neq 0$, where N is the total number of PE in the image, k_j is the number of PE in the j^{th} cell and q is the order of the fractal moment. If the Cerenkov image exhibits a self similar behavior the fractals moments G_q show a power law relation of the parameter of the length scale M: $G_q \propto M^{\tau_q}$ The exponent τ_q is determined from G_q by using the formula $\tau_q = \frac{1}{\ln 2}\frac{d\ln G_q}{d\nu}$. The slope has been obtained from $\nu = 1$ to $\nu = 4$. This exponent τ_q is related to the generalized multifractal dimensions, D_q by $D_q = \frac{\tau_q}{q-1}, q \neq 1$, where q is the order of the moment and varies over the range -6 $\leq$ q $\leq$ 6. For $q = 1$, D_1 is defined as equal to one. The value of $D_{q_{max}}$ characterizes the location and the size of the largest irregularity in the image structure. This means that, more regular the image, the closer is D_6 to 1. A more detailed description of this procedure is given in (Haungs et al. 1999). In Figure 2, we compare the distributions of the multifractal dimension D_6 for the four progenitor species comprising the data-base used in the present work. D_6 reflect the overall regularity of the image structure. As γ-ray images produce the most regular images amongst the four particle types considered here, D_6 have the largest peak values for γ-ray progenitors. Iron images are more regular than proton images, since, for the same total energy per nucleus, iron events have lesser energy per nucleon. This results in a smaller interaction length for iron primaries (as in the case of γ-rays) and hence more secondaries with lesser energy for particle than what is expected in the case of proton events. This leads to destroy a visible hadronic core in the image of an Iron progenitor, while it survives in the case of a proton image.

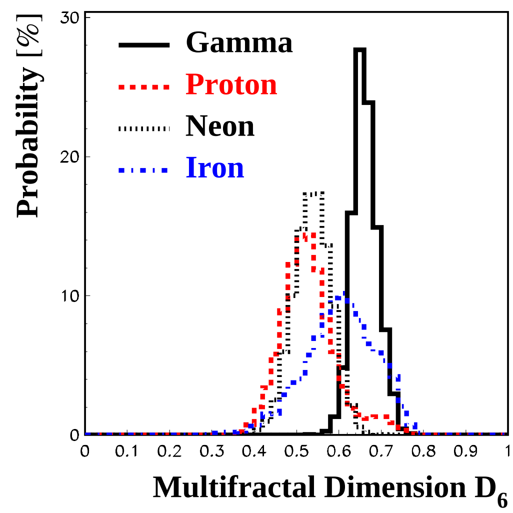

Figure 2: Distributions of the multifractal dimension D_6 for all simulated images in the range of PE from 1800 to 3000 for the different progenitor particles of the ACE.

4.2 Wavelets: A pattern analysis in terms of wavelets can be regarded as a sequence of filtering processes in order to examine the presence of local structures on different scale-lengths. In some aspects it is a generalization of a Fourier analysis, using localized functions, called wavelets instead of sine and cosine functions. When applied to the TACTIC images, the wavelet moment (Kantelhardt, Roman and Greiner 1995) W_q is used, given by: $W_q(M) = \sum_{j=1}^{M-1}(\frac{|k_{j+1}-k_j|}{N})^q$; k_j is the number of PE in the j^{th} cell in a particular scale. The wavelet moments have been obtained by dividing the Cerenkov image into $M = 4, 16, 64, 256$ equally sized parts and counting the number of photoelectrons in each part. The difference of probability in each scale gives the wavelet moment. Again a proportionality $W_q \propto M^{\beta_q}$ is given for the electron distribution in the Cerenkov images. The two wavelet dimensions which we have used for examining the structures of the Cerenkov images are the slopes β of the best-fit regression line for the double logarithmic distribution W_q vs. M for $q = 2$ and $q = 6$ obtained for each image. Figure 3 gives the distribution of the wavelet parameter β_6 for the simulated data-bases

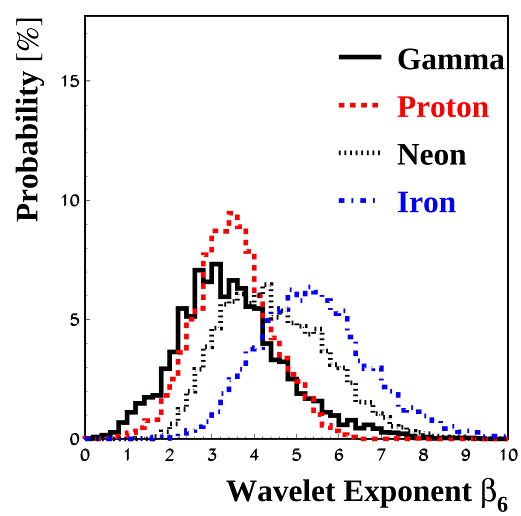

Figure 3: Distributions of the wavelet parameter β_6 for the same images as in Fig.2.

associated to the 4 progenitor species used in this work. It is well known that wavelet moments are sensitive to differences in the average numbers of photoelectrons in neighboring pixels on different length scales. With vanishing differences, i.e. regular images, the the slope of the best-fit (lnW_q vs. lnM) regression line gets flatter. As Fe and Ne events are associated with a relatively larger number of muons compared with proton (and γ-ray) events, the Cerenkov images produced by these high Z nuclei are characterized by local intensity peaks, resulting in higher values for the slope parameter in case of high Z nuclei compared with protons (and γ-rays). This feature, which may be present in the structure of a Cerenkov image, is not exploited as source of information by the use of Hillas parameters.

5 Artificial Neural Network-based Classification

We use the well known pattern recognition capabilities of an artificial neural network (ANN), in order to display the degree to which extent the event-classification potential of the fractal and wavelet parameters can be used. From a statistical modeling point of view, the ANN technique represents a non-parametric event classification scheme. Two hidden layers were used with backpropagation mode in this exercise alongwith optimized learning parameters. A sample of 12000 events was used in the training steps of the network, and the output values demanded are 0.0 for γ-rays, 0.33 for protons, 0.67 for Neon nuclei and 1.0 for Iron nuclei. The test data set comprises a total of 24000 events, belonging to γ-ray, proton, Neon and Iron species, all 4 in an equal proportion. The network was trained with two fractal (D_2 and D_6) and two wavelet (β_2 and β_6) parameter values as inputs to the net. It is clear from Figure 4 that γ-rays and hadrons are well separated, but the protons and Neon display overlapping distributions while Iron is very well separated.

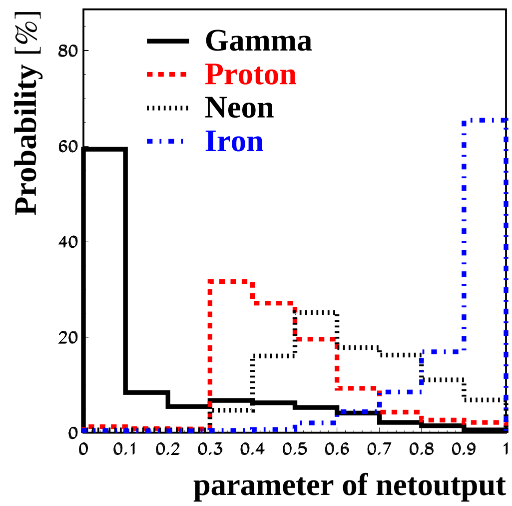

Figure 4: Distributions of the different primaries in the output parameter of a neural net analysis.

6 Conclusions

It has been shown that Cerenkov images have a fractal structure. Multifractal dimensions and wavelet moments can be used along with Hillas parameters to discriminate more efficiently amongst gamma-rays, protons, Neon and Iron progenitor species through a properly-trained artificial neural net. The multifractal and wavelet approach for analyzing Cerenkov images has been discussed for the first time in context of gamma-ray astronomy. This (preliminary) work suggests the prospects of the resulting discrimination parameters as supplementary classifiers for cosmic-ray mass-composition studies in the UHE bracket is quite promising.

References

Aharony, A. 1994, Physica A 168, 479
Bhatt, N. et al. 1999, Proc. 26th ICRC (Salt Lake City, 1999), OG 2.4.20
Haungs, A. et al. 1999, submitted to Astrop. Phys.
Heck, D. et al. 1998, FZKA-Report 6019, Forschungszentrum Karlsruhe, Germany
Kantelhardt, J.W., Roman, H.E. & Greiner, M. 1995 Physica A 220, 219